

Effect of Dual Phase Steel Processing Conditions on the Microstructure and Mechanical Properties

Ahmed Refaee¹, Sabbah Ataya^{2,3} and Samir Ibrahim²

¹ Ezz Aldekhela (EZDK) Steel Company, Alexandria, Egypt

² Department of Metallurgy and Materials Engineering, Faculty of Petroleum and Mining Engineering, Suez University, 43721, Suez, Egypt

³ Department of Mechanical Engineering, College of Engineering, Al Imam Mohammad Ibn Saud Islamic University, Riyadh 11432, Saudi Arabia

Abstract

The advantages of dual phase steels in structural applications and automobile industries motivate further studies on the effect of processing parameters on the properties of dual phase steel. Production trials of DP steels were performed using a thin slab caster (TSC). Dual phase steel with the composition (in wt. %) of 0.057 C, 0.277 Si, 1.38 Mn, 0.027 Nb, 0.036 P, 0.63 Cr 0.39 Al was produced in sheet thickness of 3.2 mm. The effects of deformation at inter-critical temperatures (790 and 800°C), coiling temperatures (120, 150 and 180°C) and cooling rate (113~136 °C/Sec) on the final microstructure were investigated. Characterization of the dual phase steels mechanical properties was carried out using hardness, quasi-static tensile test, high strain rate tensile tests, and impact tests. The final mechanical properties were correlated with the different microstructure constituents. The effect of martensite content on deformation and fracture was investigated.

Keywords

Dual phase steel; cooling regime; mechanical properties; martensite volume fraction; high strain rate tensile and fracture feature.

Introduction

Dual Phase (DP) steels have an excellent combination of strength and ductility which allows good ability for producing complex shapes. Dual Phase steels have become the preferred material in automotive and structural applications among all advanced high strength steels (AHSS). In many cases DP steels are used in most parts of car chassis, rims, desks, and sheets of the body. The high commercial potential of the newly developed alloy has motivated extensive research in numerous laboratories, resulting in DP-grades which have a wide range of chemical compositions and which are produced with various processing routes [1].

Dual-Phase (DP) steels composed of martensite islands dispersed in a ductile ferrite matrix were developed to provide a good balance between strength and ductility. In order to reach this goal, it is of prime necessity to control their final microstructure, in particular, phase volume fraction, carbon composition and banded structure [i]. The high-strength and good formability characteristics of high strength steels (e.g. Dual phase steel) when compared to conventional grades make them attractive in applications involving high rates of

loading combined with a demand for low weight. Typical examples include light-weight protective systems, crashworthiness of automotive and aerospace structures, and high-speed machining [ii]. These properties are only possible through the appropriate controlled rolling followed by controlled cooling to the coiling temperature. Both parameters should be designed in function of the steel chemical composition.

The resulted mechanical properties changes are associated with different strengthening mechanisms [iii]. In low carbon DP-steel, the carbon strengthening mechanism is partly substituted by grain refinement through controlled rolling treatment in addition to martensite phase strengthening. It is established that martensite volume fraction, size and distribution have a significant influence on the properties of the produced steel [iv].

Present work aims to focus on production evaluation of on-line trials to study the effect of the processing parameters, mainly cooling and coiling conditions on the microstructure and subsequently on steel mechanical behaviors.

Experimental Procedures

Online Production of DP Steel

Dual phase steels produced in this study were processed at EZDK (by Steel Making, Thin Slab Casting and Hot Strip Mill). The chemical composition of the used low carbon heat is shown in **Table 1**. Based on the online pyrometer temperature measurements, the production line length and the rolling speed, the cooling regime were determined as shown in **Figure 1**. The rolled sheet temperature after the finishing rolling stand ranged between 800 and 790°C. The rolled sheet was cooled down to a temperature of 680 °C, then a holding time of 3 - 5 sec in air was applied before the final cooling step to reach the coiling temperature which had changed in this work to be 120, 150 and 180°C. The cooling rate was calculated as shown in **Table 2**.

Table 1 Chemical composition (in Wt%) of dual phase steel materials.

C	Si	Mn	P	S	Cr
0.057	0.277	1.38	0.0036	0.002	0.63
Ni	Cu	Nb	Ti	Al	N
0.02	0.04	0.027	0.01	0.05	0.0049

Table 2 Cooling regime data of the dual phase steel production trials (Figure 1).

Trial No.	Finishing rolling temp. (°C)	Holding time at 680°C (sec)	Cooling time after 680°C (sec)	Cooling rate (°C/sec)	Coiling temp. (°C)
DP1	800	4.68	4.94	113.26	120
DP2	800	3.78	4.01	132.29	150
DP3	790	3.52	3.67	136.36	180

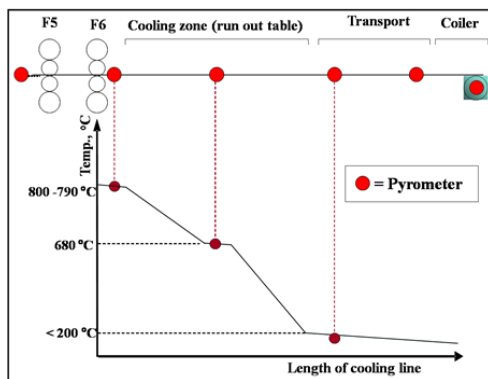


Figure 1 Applied cooling regime for dual phase production.

Materials Characterization

Quasi-static tensile tests were carried out on samples according to JIS Z2241 (specimen width of 33 mm and length of 50 mm), using the tensile testing machine Model Zwick/Roll (250 KN).

High strain rate tensile tests ($\epsilon \sim 1000 \text{ s}^{-1}$) were carried out using the Spit Hopkinson Pressure Bar [v]

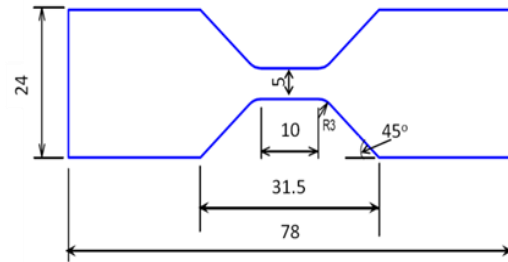


Figure 2 High strain rate tensile specimens (all dimensions are in mm).

Hardness test was conducted on the DP steels according to ASTM E 18-08b using Rockwell Hardness Tester Type Zwick, Model 3106 using the scale HRB.

Impact test was carried out according to EN 100045-1 using the sub-size specimen with a thickness of 2.5mm and a width of 10 mm with a notch depth of 2 mm. Impact tests were conducted on the different DP steels at different test temperature of RT, -20, -30, -40, -50, -60 and -70°C. Impact testing machine Type RKP 300/450 was used.

Microstructure

Samples were taken from sheets cross section perpendicular to rolling direction. The polished specimens were pre-etched in methyl alcohol Nital (2% nitric acid) for 5 sec. then rinsed in distilled water and etched for 20 sec. in 8 g Na_2SO_4 + 100 ml water according to ASTM E407-07. Microstructure was captured using an Olympus optical microscope and the grain size was measured according to ASTM E112. Martensite area fraction was also measured. SEM was also used to investigate the microstructure and the fracture surface of the various tested samples. SEM Type JEOL model JSM 5410 was used.

Results and Discussions

Micro Structural Analysis

The dual-phase steel was produced by rolling at the intercritical temperature of 890°C and holding for 3 - 5 seconds at 890°C before the final cooling to the coiling temperatures of 120, 150 and 180°C, i.e. different estimated cooling rates of ~ 113 , 132 and 137°C/sec. The finishing rolling temperature was kept constant at 800°C. The observed microstructures shown on (Error! Reference source not found. a, b and c) consisted mainly of ferrite and martensite. The measured martensite area fractions appeared to increase with increasing the coiling temperature and to vary in the range of 30 to 35% as a function of coiling conditions,

Figure 3 Microstructure of the processed dual phase steel: Martensite area fractions: a) DP1 = 0.306, b) DP2 = 0.32 and c) DP3=0.35.

Table 3 Martensite area fraction and hardness of DP steels.

The ferrite carbon content can be estimated by assuming that at quenching temperature the ferrite keeps its carbon content at the intercritical temperature. Therefore, the ferrite will be

supersaturated in carbon, with a carbon content estimated to be ~ 0.02 Wt.%. Inserting this value in Eq. (1) yields a martensite content C_m of 0.141 Wt.% C at $V_m \approx 0.306$ which decreases to 0.125 Wt. %C at the higher V_m of 0.35.

Moreover, in a low carbon steel, the crystal structure has a low degree of tetragonality (c/a ratio), compared with a higher value in a high carbon steel. The degree of tetragonality has been shown to increase linearly with the carbon content and is given by []:

$$c/a = 1.005 + 0.045 C(\text{wt}\%) \quad (2)$$

Using this equation, values of c/a equal to 1.0134 and 1.012 for MVF of 0.306 and 0.35 are obtained respectively. This will give a unit cell volume difference of 2.77% due to the increased martensite volume fraction. Subsequently, these volume differences could have an effect on the surrounding ferrite matrix. Therefore, a higher dislocation density is expected at the ferrite martensite interfaces in order to accommodate this volumetric expansion. The martensite volume expansion has been estimated to be 2.9 – 4% at the martensite starting temperature [].

Deformation under quasi-static tensile test

The engineering stress-strain curves of DP steels with MVFs of 0.306, 0.32 and 0.35 obtained with different cooling rates are shown in **Error! Reference source not found.-a**. The three curves show a continuous yielding behavior without appearance of the Lüders band. It has been reported that a minimum of 4% martensite is needed to achieve a continuous yielding []]. The specific mechanical properties changes are also shown in **Error! Reference source not found.-b** as a function of the MVF. These results indicate that there is a continuous rise in both yield stress and tensile strength with increasing martensite volume fraction which is accompanied by a decrease in the uniform strain and total elongation. This increase in strength could be attributed to a possible decrease in the strain hardening rate with increasing MVFs which will also accelerate the onset of necking the uniform strain.

In the elastic region of stress-strain curve, it is to be expected that there will be no stress transfer between the martensite and ferrite phases, because the elastic modules of both phases are almost the same. Moreover, it is generally accepted that in the easy stage of DP steel plastic deformation, yielding starts in the soft ferrite, while the hard martensite remains in the elastic state. As the strain increases, the internal stress could be expected to pile-up at the ferrite-martensite interface due to strain incompatibility between martensite and ferrite. At a further higher strain, hardening will be due to rapid dislocations multiplication and back stress resulting from the phase strain incompatibility. It has been reported that the martensite phase will start to deform plastically generally at a relatively small strain []. The onset of plastic deformation can be estimated from the stress-strain relation, where the work hardening behavior rate can be divided into three

regions; (i) initially work hardening rate is the highest of all, (ii) a gradual decrease in work hardening rate as a deformation advance and (iii) a rapid drop in the work hardening rate [ix].

Strain hardening exponent (n) is usually considered as a good indication of work hardenability of the material. The larger the n -value, the more the material can deform before instability is reached. $\ln(\sigma')$ vs $\ln(\rho)$ diagram for two different DP steel volume fractions are shown in **Figure 5**

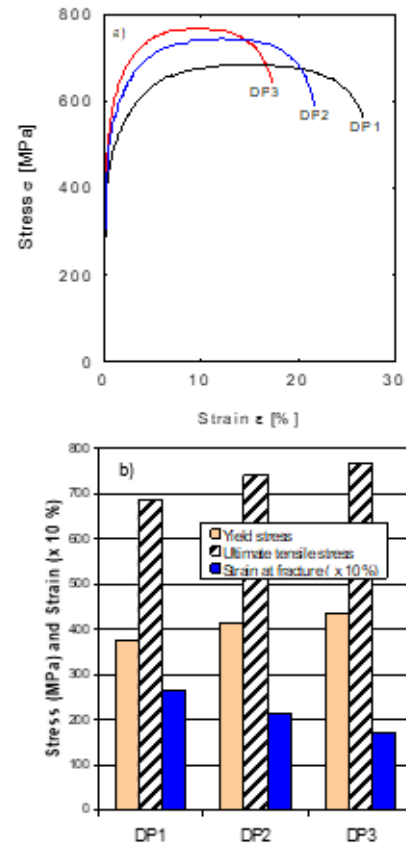


Figure 4 Tensile properties of the processed dual phase steels.

Nominally, the area fraction was described as approximately equal to the martensite volume fraction (MVF). The average ferrite grain size was measured to be around $5 \sim 6 \mu\text{m}$ and only slight changes were observed with changing the martensite volume fraction difference.

The strength difference between ferrite and martensite phase is expected to generate further dislocations at the interface zones during plastic deformation. The stress magnitude due to the two phases incompatibility will depend on the hardness difference between the hard martensite and the soft ferrite. The hardness of martensite particles is related

to its carbon content. As for the different martensite volume fraction in the steel, the change of the carbon content in the martensite phase can be estimated by the following equation:

$$C_m = \frac{C - (1 - V_m)C_f}{V_m} \quad (1)$$

Where C is the carbon content of the steel and V_m is the volume fraction of martensite in the microstructure and C_f is the ferrite carbon content

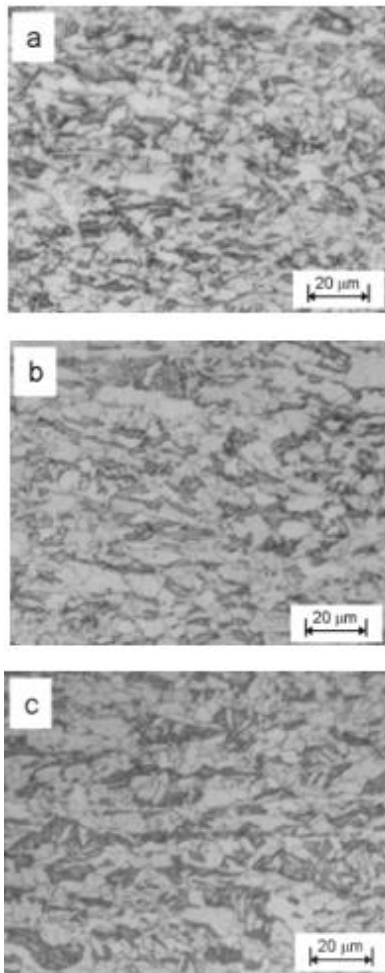


Figure 3 Microstructure of the processed dual phase steel: Martensite area fractions: a) DP1 = 0.306, b) DP2 =0.32 and c) DP3=0.35.

Table 3 Martensite area fraction and hardness of DP steels.

Trial No.	Cooling rate (°C/sec)	Coiling temperature (°C)	Martensite area fraction (%)	Rockwell hardness (HRB)
DP1	113.26	120	30.6	90
DP2	132.29	150	32	94
DP3	136.36	180	35	96

The ferrite carbon content can be estimated by assuming that at quenching temperature the ferrite keeps its carbon content at the intercritical temperature. Therefore, the ferrite will be supersaturated in carbon, with a carbon content estimated to be ~ 0.02 Wt.%. Inserting this value in Eq. (1) yields a martensite content C_m of 0.141 Wt.% C at $V_m \approx 0.306$ which decreases to 0.125 Wt. %C at the higher V_m of 0.35.

Moreover, in a low carbon steel, the crystal structure has a low degree of tetragonality (c/a ratio), compared with a higher value in a high carbon steel. The degree of tetragonality has been shown to increase linearly with the carbon content and is given by [vi]:

$$c/a = 1.005 + 0.045 C(\text{wt}\%) \quad (2)$$

Using this equation, values of c/a equal to 1.0134 and 1.012 for MVF of 0.306 and 0.35 are obtained respectively. This will give a unit cell volume difference of 2.77% due to the increased martensite volume fraction. Subsequently, these volume differences could have an effect on the surrounding ferrite matrix. Therefore, a higher dislocation density is expected at the ferrite martensite interfaces in order to accommodate this volumetric expansion. The martensite volume expansion has been estimated to be 2.9 – 4% at the martensite starting temperature [vii].

Deformation under quasi-static tensile test

The engineering stress-strain curves of DP steels with MVFs of 0.306, 0.32 and 0.35 obtained with different cooling rates are shown in **Error! Reference source not found.-a**. The three curves show a continuous yielding behavior without appearance of the Lüders band. It has been reported that a minimum of 4% martensite is needed to achieve a continuous yielding [viii]. The specific mechanical properties changes are also shown in **Error! Reference source not found.-b** as a function of the MVF. These results indicate that there is a continuous rise in both yield stress and tensile strength with increasing martensite volume fraction which is accompanied by a decrease in the uniform strain and total elongation. This increase in strength could be attributed to a possible decrease in the strain hardening rate with increasing MVFs which will also accelerate the onset of necking the uniform strain.

In the elastic region of stress-strain curve, it is to be expected that there will be no stress transfer between the martensite and ferrite phases, because the elastic modules of both phases are almost the same. Moreover, it is generally accepted that in the easy stage of DP steel plastic deformation, yielding starts in the soft ferrite, while the hard martensite remains in the elastic state. As the strain increases, the internal stress could be expected to pile-up at the ferrite-martensite interface due to strain incompatibility between martensite and ferrite. At a further higher strain, hardening will be due to rapid dislocations multiplication and back stress resulting from the phase strain incompatibility. It has been reported that the martensite phase will start to deform plastically generally at a relatively small strain [ix]. The onset of plastic deformation can be estimated from the stress-strain relation, where the work hardening behavior rate can be divided into three regions; (i) initially work hardening rate is the highest of all, (ii) a gradual decrease in work hardening rate as a deformation advance and (iii) a rapid drop in the work hardening rate [ix].

Strain hardening exponent (n) is usually considered as a good indication of work hardenability of the material. The larger the n -value, the more the material can deform before instability is reached. $\ln(\sigma')$ vs $\ln(\phi)$ diagram for two different DP steel volume fractions are shown in **Figure 5**

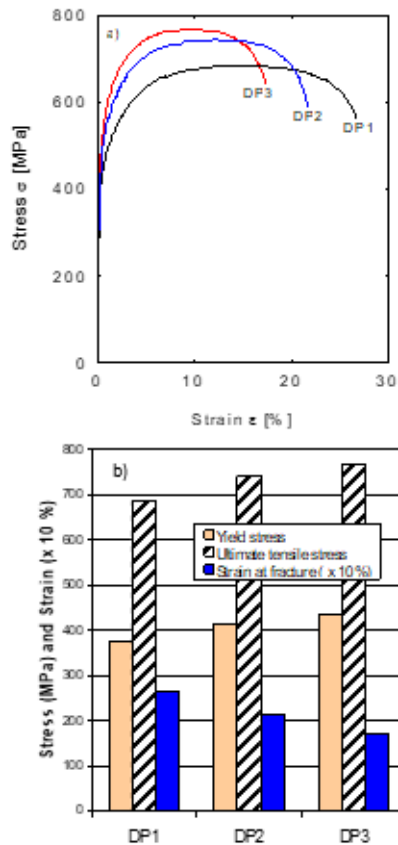


Figure 4 Tensile properties of the processed dual phase steels.

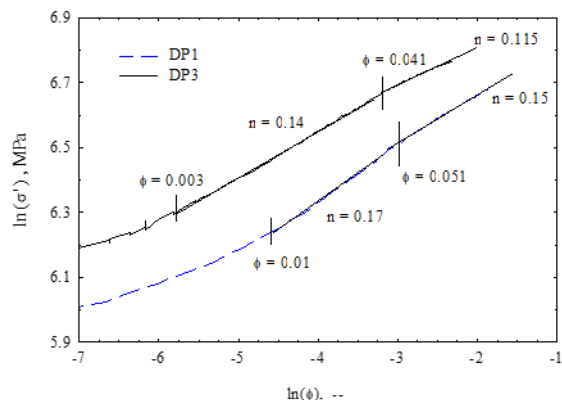


Figure 5 $\ln(\sigma')$ against $\ln(\phi)$ showing different strengthening coefficients.

In this DP-steel, strain hardening exponent of the first stage is higher than the second stage, n values are 0.14 and 0.115 for steel with 30% MVF. At a higher martensite volume fraction, the n -value changes to a higher volume of $n=0.17$ and 0.15 for the two stages. The presence of two stages of work hardening can be related to the activation of different work hardening mechanisms. The higher work hardening stage can be related to the ferrite plastic deformation, while the lower working hardening value represents the deformation of both ferrite and martensite phases. The difference between the two curves could be attributed to both differences in MVF as well as the difference in the martensite strength. The transition point between the first and second stage of work hardening could be the strain at which the martensite starts to be deformed plastically which is equal to 0.04

martensite and increased to a higher value of 0.05 strain with increasing the martensite volume fraction. Moreover, tensile results indicated that the decrease in the uniform strain with the increase of MVFs could be interpreted as being the results of an early deformation of martensite which is directly related to higher accumulated stresses at ferrite-martensite interface.

For the three martensite volume fractions, the microstructure of a uniformly deformed part of the tensile samples can be represented by the micrograph in Figure 6; the martensite appeared deformed in this zone before the start of necking. Figure 6 also shows that both ferrite and martensite grains are elongated and can be accompanied by lattice rotation in the direction of tensile axis. In the uniform deformation zone, several microstructure features appear such as a faint boundary substructure inside the ferrite grain pointed by arrow in Figure 6.

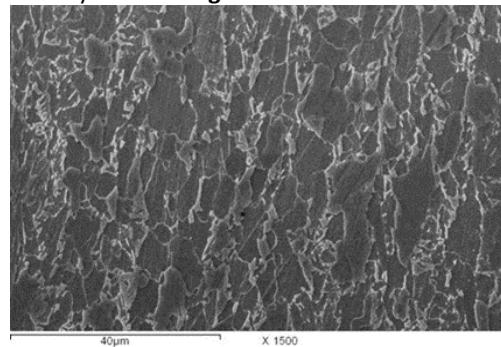


Figure 6 Uniform zone deformation (arrow indicate faint substructure boundary).

Deformation under high strain rate tensile loading.

The stress-strain curves of the various cooling rates of dual-phase steel under high strain rate of 900 to 1000 s^{-1} are shown in Error! Reference source not found.-a, b, c. The obtained homogeneous strain at maximum nominal stress values shows a small variation with changing the cooling rate, a relatively small increase at high CT conditions. Moreover, the fracture stress and the strain to fracture vary from 0.42 to 0.25% strain, Error! Reference source not found., depending on cooling rate. These changes in fracture strain could indicate the existence of different fracture modes acting and possible changes, subsequently it is expected to form ductile to semi-brittle or rather a mixed mode of fracture with a cooling rate. Such variations are not only correlated to the martensite volumes fraction, but are also due to the changes in martensitic morphology and its distribution [x]

Error! Reference source not found. shows a comparison between high strain rate tensile test and quasi-static tensile test. In high strain rate tensile tests, a higher yield stress and tensile strength are attained. The strain at fracture is also higher than that of the quasi-static tensile test. The effect of adiabatic heating under high rate of loading is clear in the high strain rate tensile test, while after reaching the ultimate tensile strength a considerable softening takes place due to possible adiabatic heat generated

during the test, as shown in **Error! Reference source not found.**

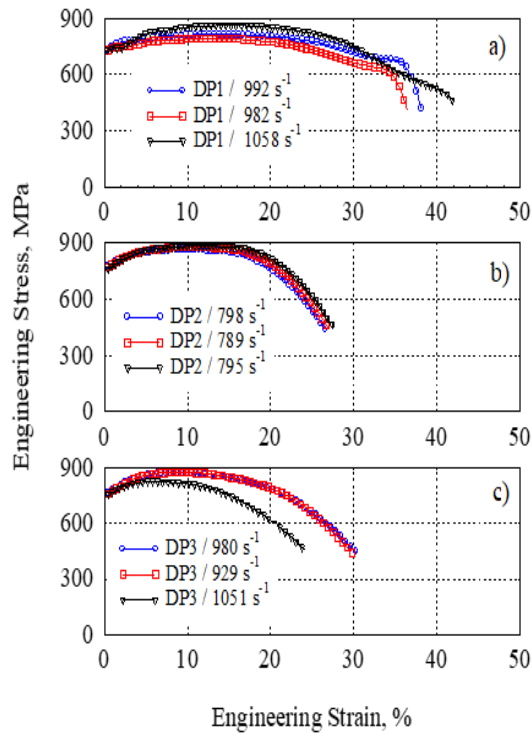


Figure 7 High strain rate tensile stress-strain curves of DP steels with cooling rates of a) 113°C/sec, b) 132°C/sec and c) 136°C/sec.

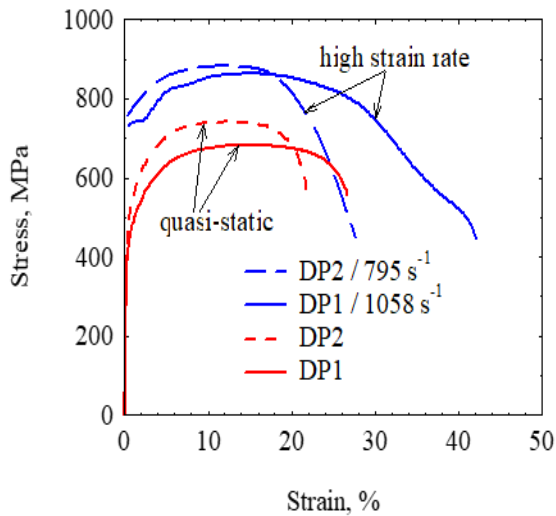


Figure 8 Quasi-static and high strain rate tensile tests for DP1 and DP2

Table 4 High strain rate tensile test conditions and results

Trial No.	Cooling rate. (°C/Sec)	Calculate d change Δ T (°C)	Strain rate (s ⁻¹)	Average Maximum Stress (MPa)	Strain at Max. stress (-)	Strain at Fracture (-)
1	113	96.9	1058	830	0.15	0.420
			982		0.15	0.357
			992		0.13	0.367
2	132	76.8	795	885	0.118	0.278
			789		0.110	0.265
			798		0.110	0.263
3	136	74.3	929	861	0.10	0.298
			980		0.10	0.303
			1051		0.08	0.250

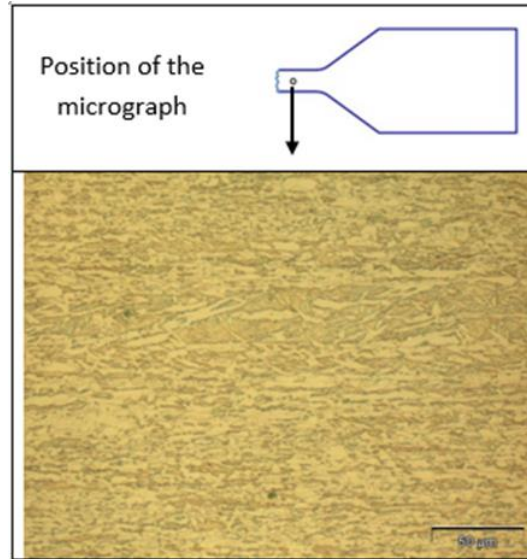


Figure 9 Microstructure of DP3 steel deformed under $\dot{\epsilon} \approx 103 \text{ s}^{-1}$

Impact tests results

Charpy impact of various cooling rates at different temperatures between -70°C to -20°C. is shown in **Error! Reference source not found.** The absorbed energy indicates a lower toughness tendency for microstructure containing a higher MFV and a relatively high temperature dependent on a lower MFV-steel. Similar results are reported for dual phase steel following impact testing [xi,xii]. However, a different mode of toughness dependent on MVF is also reported [xiii], where toughness improves with decreasing martensite phase content. Comparing different results of impact toughness could be misleading, since toughness does not depend only on MVF in DP-Steel but also on the second phase morphology, distribution of the martensite as well as on its carbon content of the martensite. A finer and dispersed more homogenous martensite will enhance the steel fracture toughness [xiv]. Grain size of the soft ferrite is not likely to contribute to toughness, since different cooling conditions resulted in small variations in grains size.

The fracture surface morphology of the different DP steels exhibits in general a typical dimple rupture, as shown in **Error! Reference source not found.** indicating ductile fracture features in addition to some cleavage facets. The dimples sizes are observed to decrease with increasing cooling rate i.e., increasing MFV. Moreover, voids are also present at the dimples junction with a relatively small size.

During impact deformation, i.e., high strain rate deformation, the soft ferrite phase deforms first leading to yielding, most probably on the tensile side of the impact specimen and further plastic deformation at a critical point, a ductile fracture is expected to nucleate [xiv]. Deep dimples with tearing ridges observed on the fracture surface could be considered as an indication of a high plastic deformation in front of the propagated cracks, while the size and depth of dimples could mainly indicate the nature of ductile fracture. The obtained good toughness of this steel with different MVF can also be

attributed to the presence of retained austenite as thin film, which is related to martensite transformation. This film can weaken the stress concentration at the crack tip during deformation [xv], with a subsequent increase of the impact energy. It is also possible that the improved toughness could partly be related to the interlocking arrangement of ferrite and martensite interface acting as effective barriers for crack arresting.

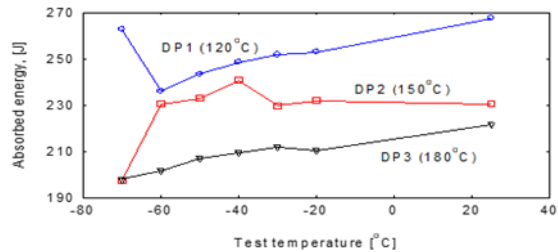


Figure 10 Absorbed impact energy of the produced dual phase steel.

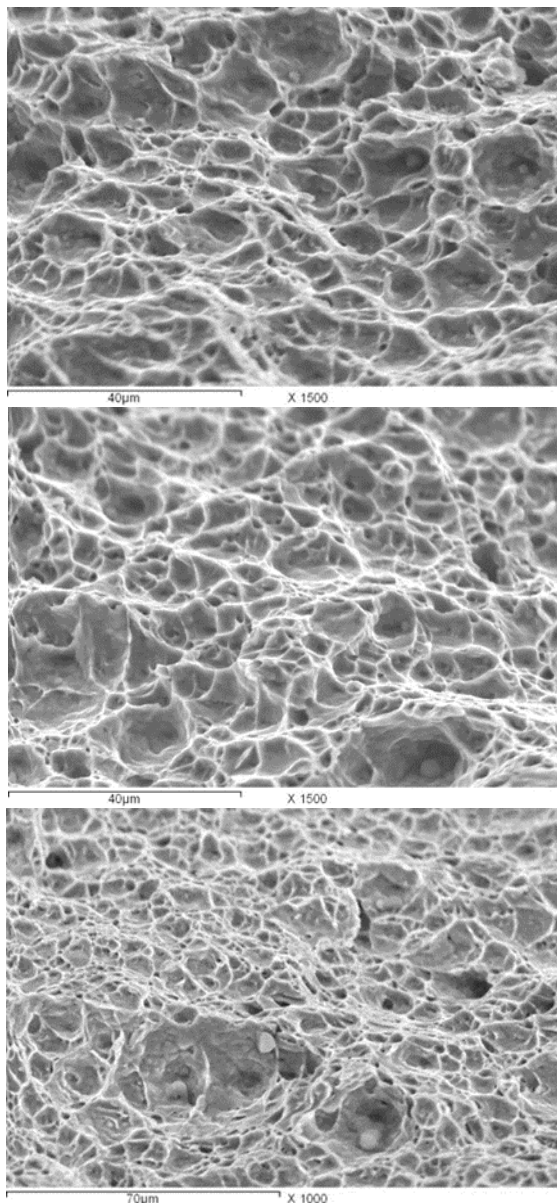


Figure 11 The impact fracture surface of different DP-steels; a) Cooling rate 113°C/Sec, b) Cooling rate 132°C/Sec and c) Cooling rate 136°C/Sec.

It was reported [xvi] that the observed cleavage facets on the fracture surface have been first explained by Kunioetal and related earlier to the occurrence of fracture of martensite. The formed microcracks of martensite impose a high shear stress on the adjacent ferrite grain leading finally to cleavage fracture of the ferrite grain.

Conclusion

Based on the results of DP steel processing trials at the conditions of the current work, it can be concluded that:

- Cooling rates are responsible for microstructures changes and three different martensite volume fractions (MVF) are obtained.
- Mechanical properties (Yield strength, tensile strength and elongation) changes are directly related to MVF for the three dual phase steels.
- Martensite starts to deform plastically during the uniform deformation stage and before necking.
- Dual phase steel has a strengthening mechanism which depends on the delicate balance between martensite carbon content, volume fraction and morphology of martensitic phase in the ferritic matrix.
- The fracture modes of the different produced dual phase steels are a mixture of ductile and brittle modes of fracture. With increasing MVF a brittle feature tendency and a reduced ductility of the steel is observed.
- During high strain rate tests ($> 790 \text{ s}^{-1}$); materials softening takes place due to the adiabatic nature of deformation. Deformation mode also shows a strong MVF dependence.

Conflicts of interest

“There are no conflicts to declare”.

References

- [1] P. Tsiouridis, Mechanical properties of Dual-Phase steel, Ph. D. (Dr.-Ing), München University (2006).
- [2] B. Krebs, A. Hazotte, L. Germain and M. Goune', Quantitative analysis of banded structures in dual-phase steel, *Image Anal Stereol*, 29 (2010), 85-90.
- [3] V. Tarigopula, O. S. Hopperstad, M. Langseth, A. H. Clausen and F. Hild, A study of localisation in dual phase high-strength steels under dynamic loading using digital image correlation and FE analysis, 45 (2008), 601–619.
- [4] N.K. Balliger, T. Gladman, Work Hardening of Dual-Phase Steels, *Metal Science*, 15 (1981), 95-108.
- [5] Denise M. Bruce, Ph. D. thesis, Dynamic tensile testing of sheet steels & influence of strain rate on strengthening mechanisms in SFIEET steels, Colorado School of Mines (2003).
- [6] M. Brodmann, Schädigungsmodeli für schlagartige Beanspruchung metallischer Werkstoffe, Ph. D. Dissertation, RWTH, Aachen University (2001), 36.
- [7] Z. Nishiyama, Martensitic Transformation, chapter 2, New York, Academic Press (1978), pp. 16-17.

- [8] T. Sakaki, K. Sugimoto, T. Fukuzato, Role of internal stress for continuous yielding of dual-phase steels, *Acta Metall.* Volume 31 (1983). 1737-1746.
- [9] M. Rigsbee, J.K. Abranam, A.T. Davenport, J.E. Frankline, J.W. Pickens, *JMS*, N.Y(1979), 304-329.
- [10] T. Pandon and T. J. Massart, *Competes Rendens Mecanique* 340 (2012), 247-260.
- [11] L.M. Dougherty, E.K. Cerreta, G.t.Gray III, C.P.Truyillc, M.F.Lope2, K.S.Vecchio, and G.J.Kusiusk, *Microstructural Development of Low-Carbon Steel and Microcomposite Steel Reinforcement Bars Deformed under Quasi-Static and Dynamic Shear Loading*, *Met and Mal Trars* 40A (2009), 1835-1850.
- [12] Y. Ahn, H. D. Kim, T. S. Byun, Y. Oh, O. Kim, J. H. Hong, *Application of intercritical heat treatment to improve toughness of SA 508 Cl.3 reactor pressure vessel steel*, *Nucl.Eng. Des.*194 (1999), 161.
- [13] N. Kim, A. H. Nagawa, *Effective grain size of dualphase steel*, *Mater. Sci. Eng.A* 83 (1986), 145.
- [14] S. Tekel, Gural. *Mat Sci. Eng A* 406 (2005), 172-179.
- [15] R. Song, D. Ponge, D. Raabe, *Mechanical properties of an ultrafine grained C-Mn steel processed by warm deformation and annealing*, *Acta Metall.* Volume 53 (2005), 4881-4892.
- [16] G. Thomas, *Retained austenite and tempered martensite embrittlement*, *Metall. Trans, A* 9A (1978), 439-450.
- [17] Y. L. Su, J. Gurland, *Strain partition, uniform elongation and fracture strain in dual phase steels*, *Mater. Sci. Eng.* 95 (1987), 151-165.
-